

Multi-model changes in El Niño teleconnections over North America in a future warmer climate

Gerald A. Meehl · Haiyan Teng

Received: 17 November 2006 / Accepted: 6 April 2007 / Published online: 5 June 2007
© Springer-Verlag 2007

Abstract Previous studies with single models have suggested that El Niño teleconnections over North America could be different in a future warmer climate due to factors involving changes of El Niño event amplitude and/or changes in the midlatitude base state circulation. Here we analyze a six-member multi-model ensemble, three models with increasing future El Niño amplitude, and three models with decreasing future El Niño amplitude, to determine characteristics and possible changes to El Niño teleconnections during northern winter over the North Pacific and North America in a future warmer climate. Compared to observed El Niño events, all the models qualitatively produce general features of the observed teleconnection pattern over the North Pacific and North America, with an anomalously deepened Aleutian Low, a ridge over western North America, and anomalous low pressure over the southeastern United States. However, associated with systematic errors in the location of sea surface temperature and convective heating anomalies in the central and western equatorial Pacific (the models' anomaly patterns are shifted to the west), the anomalous low pressure center in the North Pacific is weaker and shifted somewhat south compared to the observations. For future El Niño events, two different stabilization experiments are analyzed, one with CO₂ held constant at year 2100 concentrations in the SRES A1B scenario (roughly doubled present-day CO₂), and another with CO₂ concentrations held constant at 4XCO₂. Consistent with the earlier single model

results, the future El Niño teleconnections are changed in the models, with a weakened as well as an eastward- and northward-shifted anomalous low in the North Pacific. This is associated with weakened anomalous warming over northern North America, strengthened cooling over southern North America, and precipitation increases in the Pacific Northwest in future events compared to present-day El Niño event teleconnections. These changes are consistent with the altered base state upper tropospheric circulation with a wave-5 pattern noted in previous studies that is shown here to be consistent across all the models whether there are projected future increases or decreases in El Niño amplitude. The future teleconnection changes are most consistent with this anomalous wave-5 pattern in the models with future increases of El Niño amplitude, but less so for the models with future decreases of El Niño amplitude.

1 Introduction

It has been noted that the teleconnections over the North Pacific and North America associated with El Niño events (during northern winter when such teleconnections are strongest, associated with tropical convective heating anomalies, e.g., Branstator and Haupt 1998) could be different in a future warmer climate (Meehl et al. 1993, 2006). Meehl et al. (2006) indicated that the differences in teleconnections could be due to several factors, including changes in the amplitude of the El Niño events themselves, and an altered base state midlatitude atmospheric circulation due to the increase of greenhouse gases (GHGs) that would change the nature of the teleconnections. Those studies were performed with single models, and it remains unclear if these results could be generalized to a greater

The National Center for Atmospheric Research is sponsored by the National Science Foundation.

G. A. Meehl (✉) · H. Teng
National Center for Atmospheric Research,
PO Box 3000, Boulder, CO 80307, USA
e-mail: meehl@ncar.ucar.edu

number of models. Thus, the purpose of the present paper is to see to what extent the earlier results can be generalized to a greater number of models, and to re-visit, with these models, the relative roles of changes of El Niño amplitude and altered base state circulation.

It has been shown that there is a significant model-dependence to future changes of El Niño amplitude, with some models showing larger magnitude events, some showing smaller amplitude events, and some showing little change (Collins 2000; Merryfield 2006; Guilyardi 2005; van Oldenborgh et al. 2005; Meehl et al. 2007a). However, sampling is a significant issue in these studies since there is considerable low frequency modulation of El Niño amplitude and frequency on multi-decadal timescales in observations and models (e.g., Knutson and Manabe 1998; Meehl et al. 2006), and detecting changes of El Niño in a changing base state is a genuine challenge (Timmermann 1999). There are also differences in how the models simulate El Niño events in present-day climate (e.g., Achutarao and Sperber 2006; Capotondi et al. 2006; Guilyardi et al. 2004; Guilyardi 2005; Joseph and Nigam 2006). Therefore, physical arguments have been invoked in the studies cited above to try and explain possible future changes of El Niño from a process point of view. It has also been shown that differences in base state climate in the tropical Pacific can affect El Niño teleconnections to other regions such as Australia (Arblaster et al. 2002).

We first review the models in the World Climate Research Programme (WCRP) Coupled Model Intercomparison Project phase 3 (CMIP3) multi-model database and analyze results from the experiments with roughly doubled present-day CO₂, and quadrupled present-day CO₂. Then a subset of models are chosen, some projecting future decreases of El Niño amplitude, and some projecting future increases, to address the possible role of changes in El Niño amplitude in the manifestation of the teleconnections. Next we will examine the mean base state changes in the northern midlatitudes regarding their possible role in how El Niño teleconnections could be altered in the future.

Section 2 includes a description of the choice of models and the experiments analyzed. Section 3 looks at how these particular models simulate present-day El Niño events, while Sect. 4 examines the El Niño events in the increased GHG simulations in relation to teleconnections over the North Pacific and North America. Section 5 looks at possible effects of the mean base state changes in the models to El Niño teleconnections, and Sect. 6 presents conclusions.

2 Choice of models and experiments

There are 23 global coupled climate models (or atmosphere-ocean general circulation models, AOGCMs) in the WCRP

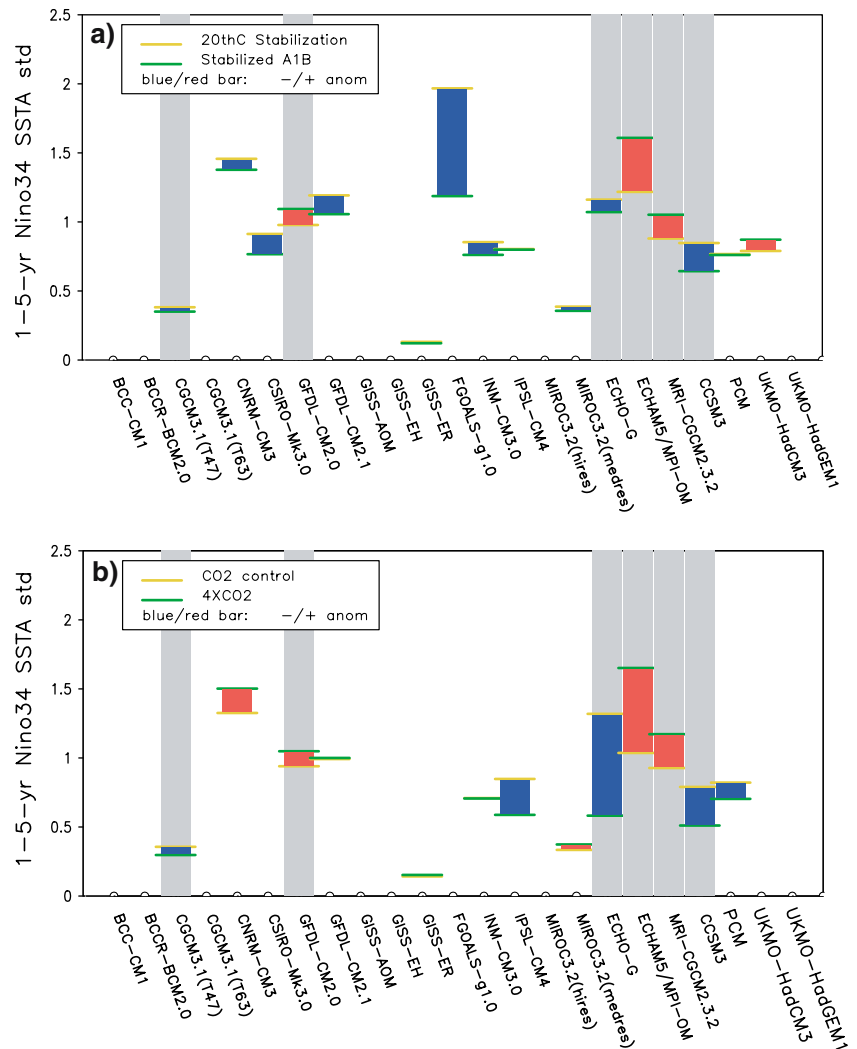
CMIP3 multi-model dataset archived at the Program for Climate Model Diagnosis and Intercomparison (PCMDI; see http://www-pcmdi.llnl.gov/ipcc/about_ipcc.php, as well as Meehl et al. 2007b, for a description). There were a variety of coordinated experiments for future climate change performed by these models, but some groups did not complete the full set. For our analyses here, we want to look at El Niño teleconnections in stabilized experiments with two different future forcings, one with roughly doubled CO₂ and another with quadrupled CO₂. For the former, we choose the A1B experiment, an intermediate magnitude forcing scenario where GHGs increase from year 2000 to 2100 until CO₂ is roughly double present-day values, and then concentrations of GHGs are held constant and the models are run for an additional 100 years with those stabilized concentrations (e.g., Meehl et al. 2005). Though concentrations are stabilized, the climate system is still slowly changing due to climate change commitment. Therefore, we compare the climate changes in the stabilized A1B experiment to the commitment experiment where concentrations were held constant at year 2000 values and the models were then run an additional 100 years, and we compare the 100 years of year 2000 stabilization to the 100 years of A1B stabilization.

For the higher forcing, an idealized forcing experiment was performed where the models branched from a control experiment, and then CO₂ was increased at 1% per year. When CO₂ reached four times present-day amounts, concentrations were held constant and the models were run an additional 100 years. For these experiments, we compare the 100 years of stabilized 4XCO₂ with 100 years from the control run.

Results shown here for all experiments use non-detrended model data, though detrending does not change the results appreciably.

In examining the models in the CMIP3 dataset, it became apparent that all models did not run both of these experiments (Fig. 1). For the stabilized A1B experiment, 16 out of the 23 models submitted output, and for the stabilized 4XCO₂ experiment, 13 out of the 23 models were present in the database. Since we wanted the same set of models for the two experiments, we proceeded to further examine the 13 in common between the two to determine the nature of their changes of El Niño amplitude. We calculate variances of 1–5 year bandpass filtered Niño 3.4 [averaged sea surface temperatures (SSTs) in the area 5N–5S, 170W–120W] for each experiment as the indicator of El Niño amplitude. Figure 1 shows that three of the models have consistent projected increases of El Niño amplitude in the future warmer climate in the two experiments (GFDL_cm2.0, MPI_echam5, and MRI_cgcm2.3.2), and three have consistent decreases in both experiments [CCCMA_cgcm3(T47), MIUB_echog, and NCAR_ccsm3]. Therefore, based on this compilation, we chose these six

Fig. 1 a Variances of 1-5-year filtered Niño3.4 SST anomalies from the 100-year 20th-century commitment (yellow line) and stabilized A1B (green line) scenarios. The blue/red bars indicate decrease/increase of ENSO amplitude as CO₂ level increases. **b** same as **a** except for the CO₂ control and 4XCO₂ runs. Six models that show consistent ENSO amplitude change from the two sets of experiments are gray-shaded



models to analyze possible future changes in teleconnections. As can be seen in Fig. 1, the rest of the models either have at least one of the four experiments missing, or have contradictory El Niño amplitude change.

As noted above, we define El Niño events in each experiment as a Niño3.4 December–January–February (DJF) anomaly (time series band pass filtered at 1–5 years) that exceeds one standard deviation for that model experiment for the DJF season when El Niño amplitude is greatest and thus the teleconnections to the Northern Hemisphere are largest (e.g., Meehl 1987; Yasunari 1991). Figure 2 shows the phase locking to the seasonal cycle whereby there is relatively greater Niño3.4 variability in the DJF season for the observations and the models. The year of the El Niño (year 0) is then the first calendar year the El Niño occurs (e.g., van Loon et al. 2003). For the increased amplitude models for the stabilized A1B experiment, the number of events ranges from 16 to 19, and for 4XCO₂ from 16 to 22 in the respective 100 year periods

analyzed (Table 1). For the decreased amplitude models, for A1B there are between 10 and 14 events, and for 4XCO₂ the range is 3–10. Therefore, El Niño events are less frequent in this particular set of models that have decreased amplitude events compared to the models with increased amplitude events. The drop in the number of events for the decreased amplitude models is caused not only by the weakening of the Niño3.4 amplitude during northern winter, but in a flattening of phase locking to the seasonal cycle (i.e., reduced Niño3.4 amplitude in northern winter and little change in northern summer). This is especially pronounced for the 4XCO₂ experiment for CCSM3 and ECHO-G. For the models with increased El Niño amplitude, the largest increases in Niño3.4 variability generally occur during the northern winter season, thus increasing the phase locking to the seasonal cycle (Fig. 2). Also note in Fig. 2 that the models with future decreased El Niño amplitude generally simulate the seasonal timing and magnitude of the monthly Niño3.4 variability better than

Fig. 2 Standard deviation of Niño3.4 SST by month, *solid lines* indicate reference conditions (either 20th century stabilization or control run as noted at *top of panels*), and *dashed lines* indicate future conditions (either stabilized A1B or 4XCO₂ as noted at *top of panels*) for **a** and **b** models with decreased future El Niño amplitude; **c** and **d** models with increased future El Niño amplitude. *Gray shaded bars* denote observed values for the period 1900–1999 from the HadISST1 dataset (adapted from Rayner et al. 2003)

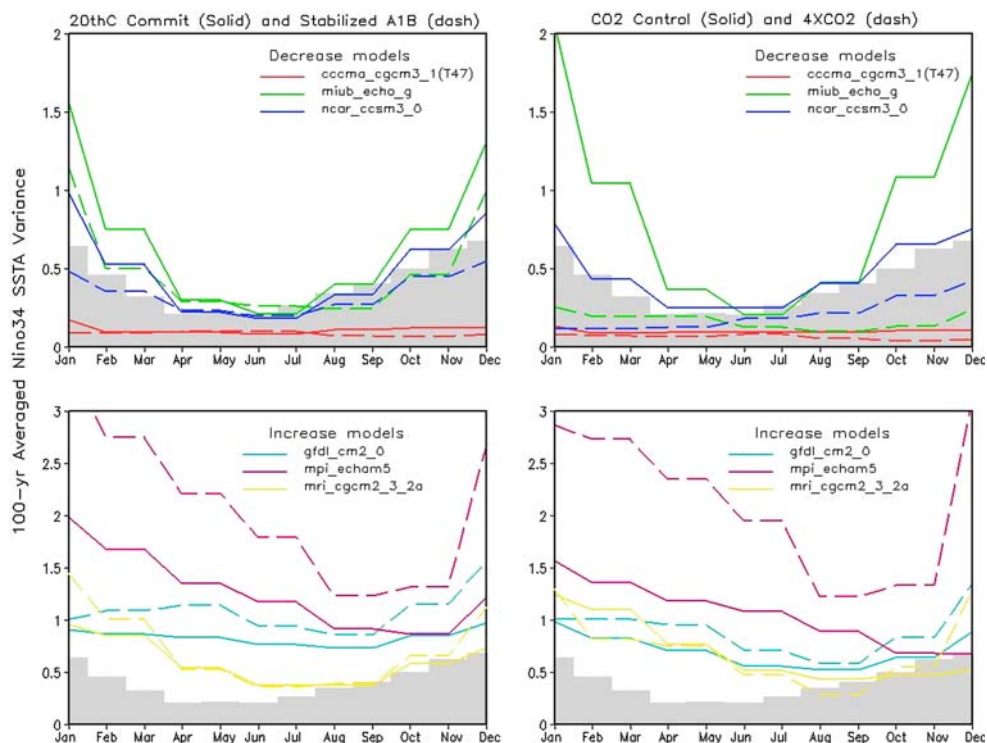


Table 1 Number of El Niño events from the six selected models

Model	20th Century stabilization	Stabilized A1B	CO ₂ control	4XCO ₂
Decrease models				
CGCM3.1(T47)	13	10	16	10
ECHO-G	19	14	24	9
CCSM3	21	14	18	3
Increase models				
GFDL-CM2.0	16	16	16	18
ECHAM5/MPI-OM	19	21	20	20
MRI-CGCM2.3.2	16	24	22	21

the models with future increased El Niño amplitude. The latter group have larger Niño3.4 magnitude in all months, and tend to shift the minimum monthly values to later in the year compared to observations. However, all models are consistent with observations in showing enhanced Niño3.4 variability during the northern winter months.

Below we compute composites across all available ensemble members for the models in order to assess the statistical significance of the changes. To check that models with more El Niño events do not influence the multi-model composites more than models with less events, we also computed single model averages before calculating the ensemble means so that each model is weighted equally. This does not appreciably change the results.

3 El Niño in the models and teleconnections

To determine the nature of the El Niño teleconnections in the models compared to the observations, Fig. 3 shows composite El Niño event anomalies of surface air temperature which, over ocean, is comparable to sea surface temperature (SST, Fig. 3a), precipitation (Fig. 3d), and sea level pressure (SLP, Fig. 3g) from the NCEP/NCAR reanalyses for the DJF season of El Niño years 0 of 1957, 1963, 1965, 1968, 1972, 1976, 1982, 1986, 1991, 1997 and 2002. For SST (Fig. 3a), the typical El Niño pattern of positive SST anomalies in the central and eastern equatorial Pacific is evident, with values over +1°C. Over North America, there are positive temperature anomalies of roughly +1°C over Canada and Alaska, and negative anomalies of around -1°C over the southern tier of states in the United States. For observed precipitation anomalies for the year 0 DJF El Niño season, there are positive anomalies in the central and eastern tropical Pacific of about 3 mm day⁻¹, negative anomalies to the northwest and southwest (Fig. 3d), positive anomalies over the west coast of the United States extending to the southeast United States, and negative anomalies over Canada and Alaska. These anomalies are associated with the SLP anomaly pattern in Fig. 3g, characterized by the familiar Southern Oscillation pattern of negative SLP anomalies over the eastern tropical Pacific, and positive anomalies over the western tropical Pacific. In the North Pacific there is an anomalously deepened Aleutian Low with maximum val-

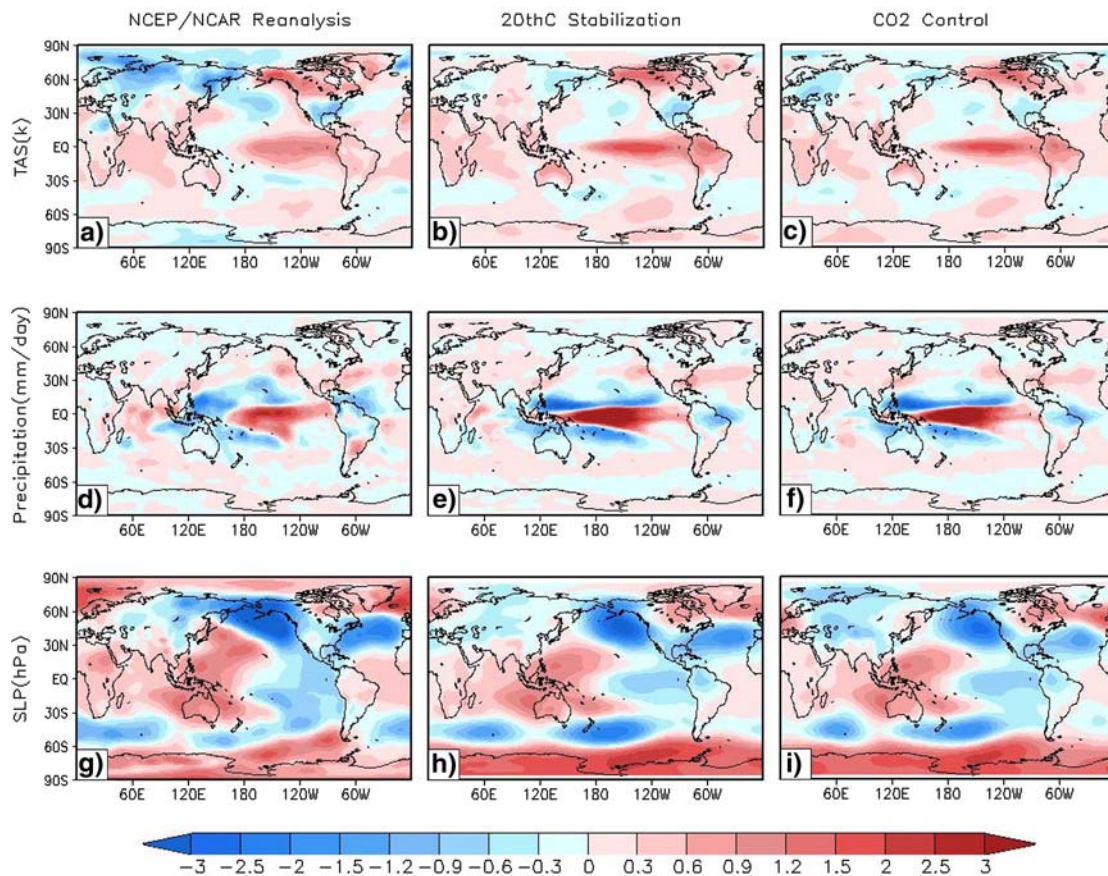


Fig. 3 **a** Surface temperature anomalies ($^{\circ}\text{C}$) for a composite of observed El Niño events, years 0 DJF minus long term mean, for the NCEP/NCAR reanalyses for events listed in the text; **b** same as **a** except for six-member multi-model composite of El Niño events from the 20th century stabilization reference experiment; **c** same as **b**

except for the present day control experiment; **d** same as **a** except for precipitation (mm day^{-1}); **e** same as **b** except for precipitation; **f** same as **c** except for precipitation; **g** same as **a** except for SLP (hPa); **h** same as **b** except for SLP; **i** same as **c** except for SLP

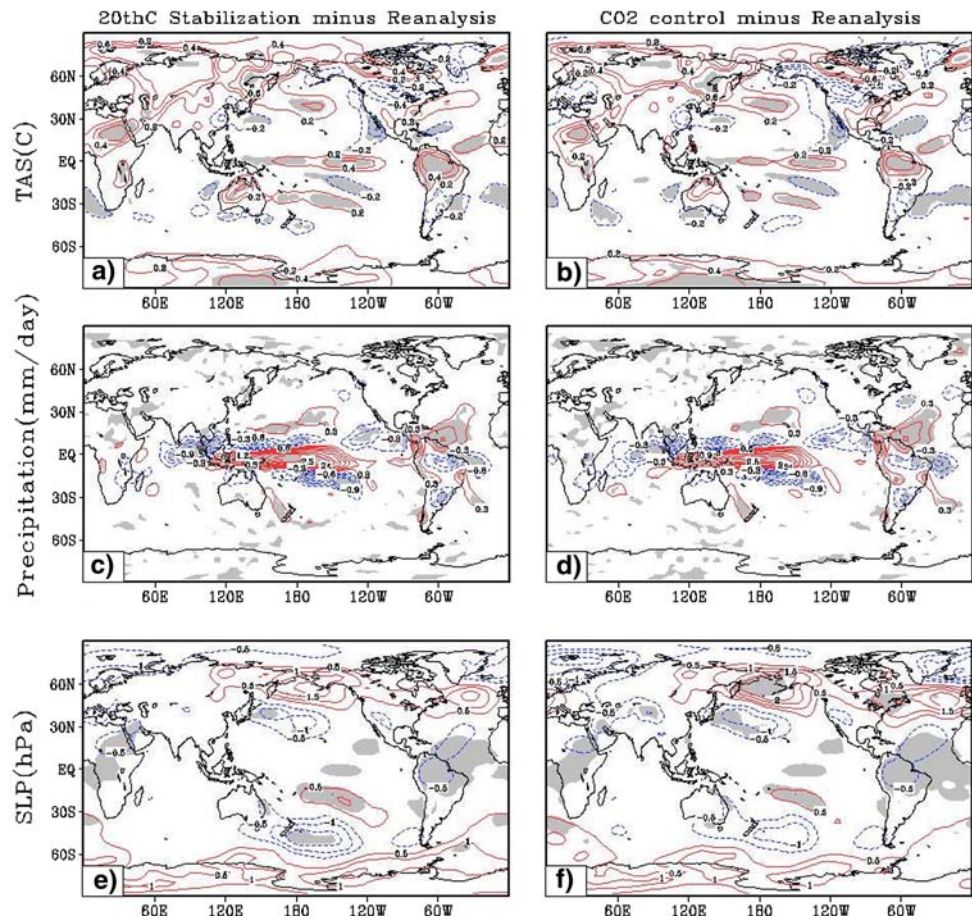
ues well over 4 hPa, and negative anomalies over the Southeast United States of over 0.5 hPa (Fig. 3g).

Comparing a six-member multi-model ensemble with the observations for the 20th century stabilization and present-day control experiments, the patterns in Fig. 3 are all qualitatively similar to the observations with specific regional differences. For example, in both model reference experiments, the positive SST anomalies in the equatorial Pacific extend too far west, reaching into the western Pacific warm pool (Fig. 3b, c). This systematic error in the El Niño SST anomaly pattern is then associated with positive precipitation anomalies that also extend too far west, reaching all the way to Papua New Guinea (Fig. 3e, f) where in observations the positive precipitation anomalies extend only to just east of the Solomon Islands (Fig. 3d). These errors are shown as differences for model composite El Niño events minus observed El Niño events (Fig. 4), with the shading indicating model errors significant at the 10% level.

The corresponding negative precipitation anomalies are squeezed to the north and south of the western Pacific warm pool in the models (Fig. 3e, f). Over North America, the positive temperature anomalies are pushed farther north into Canada and Alaska in the models compared to the observations (Fig. 3a–c), with values colder by about 0.5°C over southern Canada in the models (Fig. 4a, b). The negative temperature anomalies over the southeast United States are weaker by about 0.5°C compared to the observations (Fig. 4a, b). There are larger negative precipitation anomalies in the model simulations over the Pacific Northwest (Fig. 3e, f compared to Fig. 3d) with values further reduced by -0.3 mm day^{-1} in the models (Fig. 4c, d).

The negative SLP anomalies associated with the positive SST anomalies in the equatorial eastern Pacific are more narrowly confined to the equatorial eastern Pacific in the models (Fig. 3h, i) compared to the observations (Fig. 3g), while the anomalous negative SLP anomalies in the North Pacific

Fig. 4 **a** Differences of six-member multi-model composite El Niño events for the 20th century stabilization reference experiment minus composite observed El Niño events for surface temperature ($^{\circ}\text{C}$); **b** same as **a** except for the present day control experiment; **c** same as **a** except for precipitation (mm day^{-1}); **d** same as **b** except for precipitation; **e** same as **a** except for SLP (hPa); **f** same as **b** except for SLP. *Red solid contours* are positive differences, *blue dashed* are negative. *Shading* indicates differences significant at the 10% level



are shifted somewhat to the south and east as indicated by the positive values of about 2 hPa over the Aleutians, and negative values over the southwest United States (Fig. 4e, f). This is associated with the westward-shifted precipitation anomalies in Fig. 3e, f, indicated by the positive values of roughly 3 mm day^{-1} west of the dateline in Fig. 4c, d. An indication of the consequences of such a westward shift in the positive precipitation anomalies in the equatorial Pacific that produce a consequent westward shift in the positive convective heating anomaly in a somewhat different context are shown by Meehl et al. (2006). For a westward-shifted positive convective heating anomaly, there is a component of the anomalously deepened Aleutian Low that shifts south and east. Also, even though the multi-model ensemble mean SST anomalies in the equatorial central Pacific are somewhat stronger than the observed composite in Fig. 3a vs. Fig. 3b, c (indicating the models with stronger-than-observed El Niño variability dominate the multi-model ensemble average as noted above), the North Pacific teleconnections are somewhat weaker. However, the teleconnections are actually stronger in the Southern Hemisphere (comparing Fig. 3g to Fig. 3h, i). The latter are characterized by negative SLP

anomalies from roughly 40S to 60S, and positive anomalies south of 60S in both the observations and models. Therefore, the models capture the essential elements of the El Niño pattern and teleconnections to midlatitudes with some regional differences.

4 Changes in El Niño teleconnections

Examination of the SLP anomaly teleconnection patterns for the models that have increased and decreased El Niño amplitudes all show roughly comparable qualitative patterns to those from the model reference states and the observations depicted in Fig. 3 (not shown). However, there are subtle but important regional changes, and to identify how the teleconnections change in the model simulations, Fig. 5 shows the SLP differences, stabilized A1B minus 20th century stabilization and stabilized 4XCO₂ minus control, for the decreased El Niño amplitude models (Fig. 5a, b, respectively), increased El Niño amplitude models (Fig. 5c, d, respectively), and the six-member multi-model ensemble (Fig. 5e, f, respectively). First looking at the six-member ensemble for both stabilized

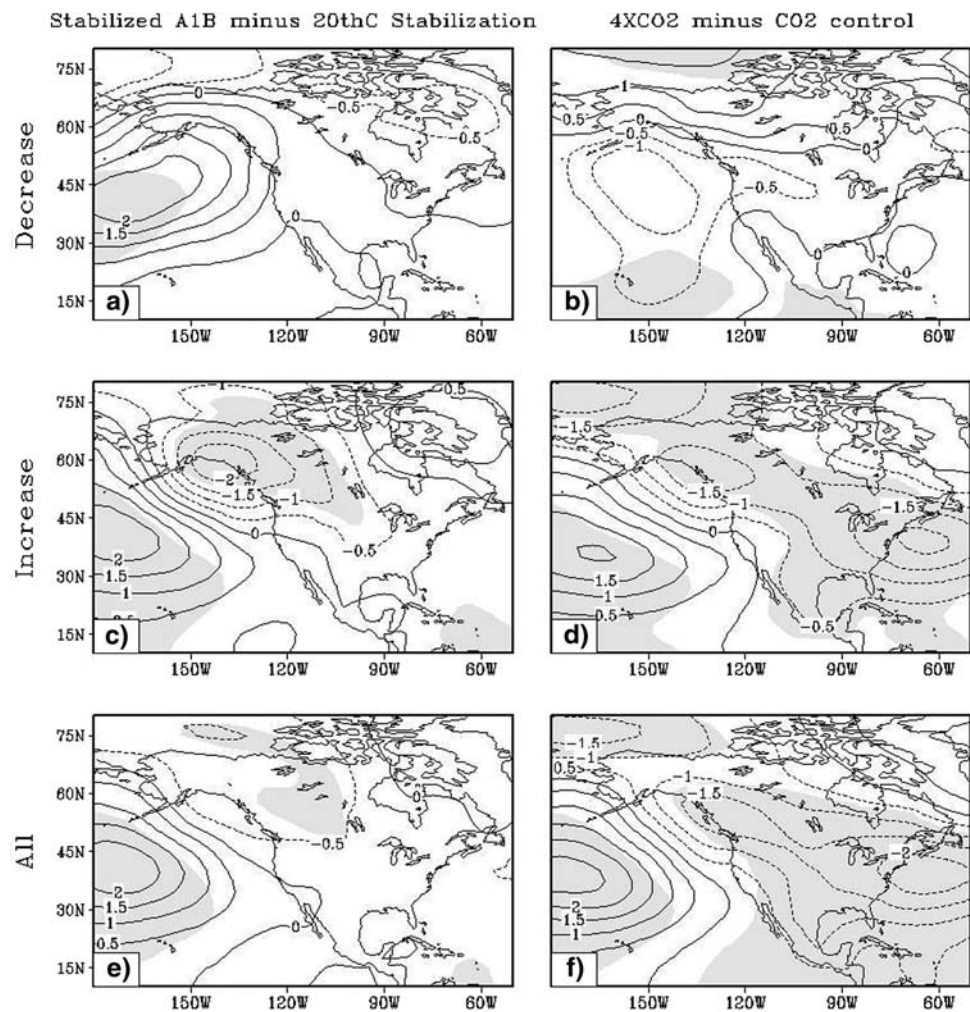
A1B and 4XCO₂ (Fig. 5e, f), an eastward and southward shift, and weakening of the anomalously deepened Aleutian Low is indicated by significant negative SLP anomalies over Canada and Alaska and positive anomalies north of Hawaii. There are larger areas of significant negative anomalies greater than -1.5 hPa over most of North America for 4XCO₂ compared to smaller differences of over -0.5 hPa for stabilized A1B (Fig. 5f). This eastward and southward shift of the anomalous low pressure in the North Pacific for future El Niño events in these six models was similar to what was noted for two models analyzed by Meehl et al. (2006). Since the models with increased El Niño amplitude have a larger response, much of this pattern seen in the multi-model ensemble is driven by changes in those three models, such that there are very similar patterns and amplitudes in Fig. 5c, d compared to Fig. 5e, f.

For the models with decreased El Niño amplitude, there are smaller amplitude changes as noted above, but for the composite as calculated here there is less of an eastward shift of the anomalously deepened Aleutian Low but still a weakening indicated by significant positive SLP anomalies

north of Hawaii for the A1B experiment (Fig. 5a). For the 4XCO₂ El Niño events for the models with decreased El Niño amplitude, there is an eastward shift but less of a weakening signified by only negative values northeast of Hawaii (Fig. 5b). Therefore, for the SLP teleconnection pattern, there is a general weakening and eastward shift of the anomalously deepened Aleutian Low in future El Niño events, with this shift stronger with greater CO₂ forcing (larger changes in the 4XCO₂ experiment compared to the A1B) in the models with future increases of El Niño amplitude. This response is weaker in the models with decreased El Niño amplitude. Therefore, the nature of the changes of future El Niño teleconnections with regards to SLP anomalies depends not only on the size of the GHG forcing, but whether models project a future increase or decrease of El Niño amplitude.

For the temperature changes associated with these changes in SLP teleconnections for the multi-model ensemble, the greater negative SLP anomaly over North America is associated with greater easterly surface flow and significantly more negative surface temperature

Fig. 5 a Differences of El Niño event teleconnections for SLP (hPa), stabilized A1B minus 20th century stabilization experiment, for the three-member composite for models with projected decreased El Niño amplitude; **b** same as **a** except for 4XCO₂ minus present-day control events; **c** same as **a** except for the three models with projected increases of El Niño amplitude; **d** same as **b** except for the three models with projected increases of El Niño amplitude; **e** same as **a** except for the six-member multi-model ensemble; **f** same as **b** except for the six-member multi-model ensemble. *Solid contours* are positive differences, *dashed* are negative. *Shading* indicates differences in El Niño teleconnections significant at the 10% level



anomalies over northern Canada and Alaska. There are maximum values of nearly -1°C over Alaska for the A1B experiment (Fig. 6e) and nearly -1.5°C over northern Canada for 4XCO₂ El Niño events (Fig. 6f). This means that the positive temperature anomalies for composite present-day El Niño events in Fig. 3b c are reduced in future events. There are also correspondingly more significant negative surface temperature anomalies over the southeast United States in the A1B experiments which make the negative temperature anomalies in present-day events (Fig. 3b, c) even colder in association with the anomalous northwesterly surface flow indicated by the changes in SLP anomalies in Fig. 5e, f. The values are cooler by about -0.2°C for A1B (Fig. 6e), and over -0.4°C in the southwest and southeast in the 4XCO₂ experiment (Fig. 6f). Thus, like the SLP, the greater the GHG forcing, the larger the changes in teleconnections with regards to temperature.

And also like the SLP plots, the temperature changes in the six model composites are driven mainly by the changes in the models with increased El Niño amplitude (note similarity of patterns in Fig. 6c, d compared to Fig. 6e, f). Correspondingly, the changes in the models with decreased El Niño amplitude are somewhat different, consistent with the changes in SLP teleconnections in Fig. 5a, b. They show temperature decreases over northwestern Canada extending down to the Pacific Northwest for the stabilized A1B experiment (Fig. 6a), while the temperature decreases occur mainly in northern Canada in the 4XCO₂ experiment, with increases over the western United States (Fig. 6b).

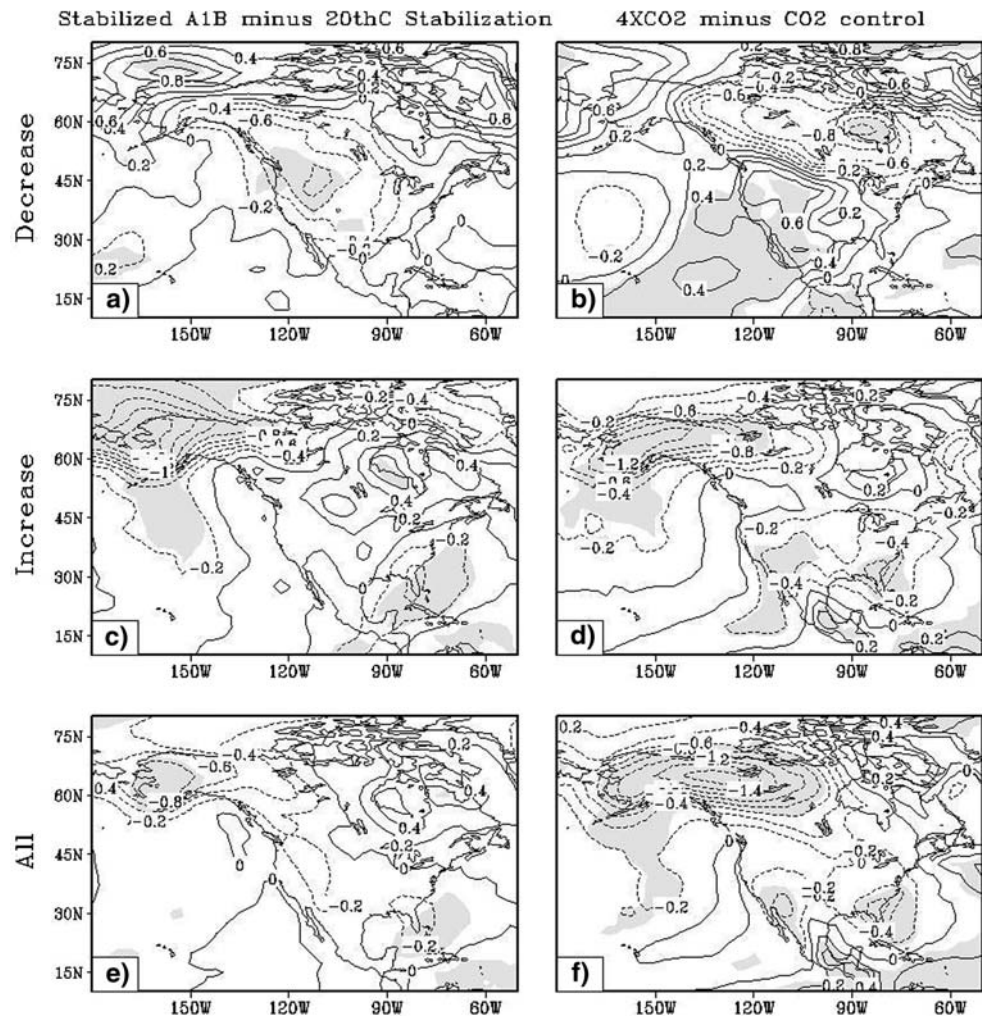
For precipitation changes in Fig. 7, the six-member multi-model ensemble shows changes again consistent with the SLP changes in teleconnections in Fig. 5, with the greater anomalous onshore flow in the Pacific Northwest producing greater rainfall there during future El Niño events, relatively speaking, compared to present-day events where there are decreases in precipitation (Fig. 3e, f). As with SLP, these six-member multi-model ensemble differences are most evident in the models with increasing El Niño amplitude, with the significant increases of precipitation during future El Niño events in relation to the present-day events of over $+0.5\text{ mm day}^{-1}$ in the Pacific Northwest (Fig. 7c, d), and some relatively smaller amplitude decreases of precipitation in areas of the southwest and southeast United States. For the decreased El Niño amplitude models, for greater forcing and the eastward shift of the north Pacific SLP anomalies, there is also a significant increase of precipitation during El Niño events in the Pacific Northwest for 4XCO₂ with values approaching $+1\text{ mm day}^{-1}$ (Fig. 7b), while there are some significant increases in precipitation in the A1B experiment in the southwest (Fig. 7a).

5 Changes in base state circulation in the northern midlatitudes

As noted in previous studies (e.g., Selten et al. 2004; Meehl et al. 2006), a characteristic in some models of the change in base state upper tropospheric circulation in the northern midlatitudes during winter with increased GHGs is a wave-5 pattern. This is seen for the five-member (ECHO-G did not supply upper level winds) multi-model ensemble in Fig. 8e, f for both the low and high forcing experiments, respectively, as well as for a larger multi-model ensemble of available model simulations (Fig. 8g, h; stippling indicates 80% of models have the same sign of response). There are negative 300 hPa streamfunction anomalies for the mean climate change near the Mideast, eastern China, North Pacific, southeast North America and eastern Atlantic. The anomaly values are larger for the greater forcing in the 4XCO₂ experiment in Fig. 8f compared to the A1B experiment in Fig. 8e. As could be expected from the results in the previous section, there are strong correspondences between the patterns in Fig. 8c, d for the models with increased El Niño amplitude and the five-member multi-model ensemble in Fig. 8e, f. However, this pattern is also evident in the models with decreased El Niño amplitude in Fig. 8a, b. This is reflected as a fundamental change in the base state midlatitude circulation (using 100 year averages for each) seen in the larger multi-model ensemble (Fig. 8g, h). Therefore, all models are showing a similar change in midlatitude upper troposphere Northern Hemisphere base state circulation whether they have future increases or decreases of El Niño amplitude. For the increased El Niño amplitude models, the eastward and southward shift of the negative SLP anomalies in the North Pacific (Fig. 5c, d) can be related to the positive streamfunction anomalies northwest of Hawaii and the negative anomalies in the Gulf of Alaska (Fig. 8c, d). However, since a similar 300 hPa streamfunction pattern emerges for the base state change for the models with decreased El Niño amplitude (Fig. 8a, b), and the character of the SLP and other teleconnection changes is somewhat different from the models with increased El Niño amplitude discussed in the previous section (e.g., Fig. 5a, b), the implication is that changes in future El Niño amplitude could make a contribution to the nature of the changes of El Niño teleconnections over North America. However, the models with increased El Niño amplitude show stronger and more consistent responses corresponding to the base state circulation change over the North Pacific and North America, pointing to the importance of changes to the base state circulation for the manifestation of future El Niño teleconnections.

As noted above, a similar and very consistent change in base state across the models (denoted by stippling where at

Fig. 6 **a** Differences of El Niño event teleconnections for surface temperature ($^{\circ}\text{C}$), stabilized A1B minus 20th century stabilization experiment for the three-member composite for models with projections of decreased El Niño amplitude; **b** same as **a** except for 4XCO₂ minus present-day control events; **c** same as **a** except for the three models with projected increases of El Niño amplitude; **d** same as **b** except for the three models with projected increases of El Niño amplitude; **e** same as **a** except for the six-member multi-model ensemble; **f** same as **b** except for the six-member multi-model ensemble. *Solid contours* are positive differences, *dashed* are negative. *Shading* indicates differences in El Niño teleconnections significant at the 10% level



least 80% of the models agree in the sign of the change) is shown for a 15-member multi-model ensemble in Fig. 8g for all models that contributed upper level winds from the 20th century stabilization and stabilized A1B experiments to the WCRP CMIP3 archive, as well as a 12-member multi-model ensemble in Fig. 8h for all models that contributed upper level winds from the control and 4XCO₂ experiments.

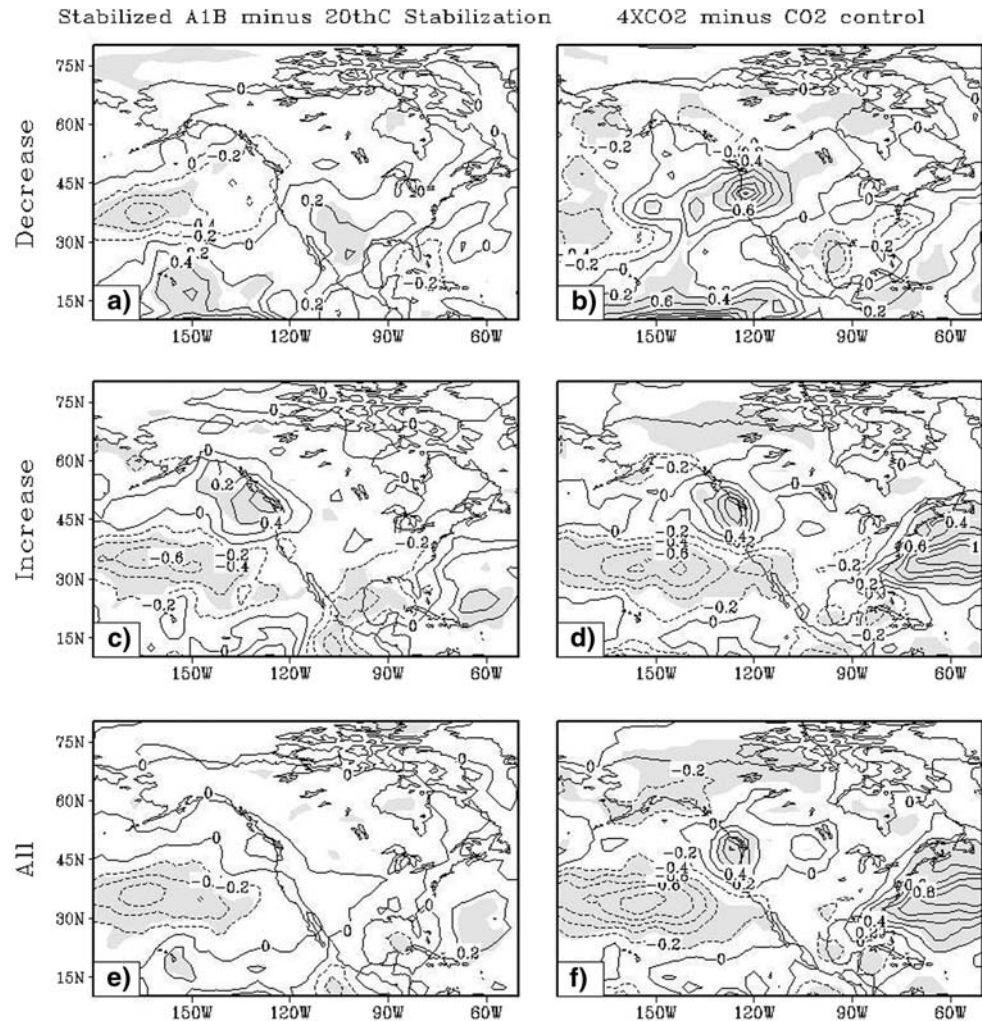
The mechanism of this change in El Niño teleconnection over North America is related to the change in future midlatitude base state circulation as shown by Meehl et al. (2006). By combining convective heating anomalies in different locations in the equatorial Pacific, with one replicating the midlatitude base state change for increased CO₂, and another representing an El Niño convective heating anomaly, the southward and eastward shift of the anomalously deepened Aleutian Low shown here in Figs. 3 and 4 was reproduced, and directly attributed to the change in midlatitude base state. Thus, the present results combined with those of Meehl et al. (2006) indicate that a

change of El Niño teleconnections over North America is directly related to the change of northern midlatitude base state circulation in a warmer climate.

6 Conclusions

Six models, three with projected future increases of El Niño amplitude, and three with projected decreases of El Niño amplitude, are analyzed with two different levels of future GHG forcing in stabilized experiments, one with relatively low forcing for about doubled present-day CO₂ (stabilized A1B), and the other with relatively greater forcing (stabilized 4XCO₂). The six-member multi-model ensemble shows good qualitative correspondence with observed El Niño anomaly patterns in terms of surface temperature, precipitation and SLP. El Niño events in the models and observations show warm surface temperature anomalies in the central and eastern Pacific equatorial Pacific, an anomalously deepened Aleutian Low, warmer

Fig. 7 **a** Differences of El Niño event teleconnections for precipitation (mm day^{-1}), stabilized A1B minus 20th century stabilization experiment for the three-member composite for models with projections of decreased El Niño amplitude; **b** same as **a** except for 4XCO₂ minus present-day control events; **c** same as **a** except for the three models with projected increases of El Niño amplitude; **d** same as **b** except for the three models with projected increases of El Niño amplitude; **e** same as **a** except for the six-member multi-model ensemble; **f** same as **b** except for the six-member multi-model ensemble. *Solid contours* are positive differences, *dashed* are negative. *Shading* indicates differences in El Niño teleconnections significant at the 10% level



surface temperatures over northern North America, colder temperatures over southern North America, less precipitation over northern North America, and greater precipitation over southern North America.

For future El Niño events, the models with both increased and decreased El Niño amplitude simulate qualitatively similar teleconnection patterns, but with important regional differences. In general, there are greater changes of teleconnection patterns with greater forcing, and stronger and more consistent changes of teleconnections in the models with increased El Niño amplitude. In these models, the future El Niño teleconnection patterns are characterized by a weakened as well as a southward- and eastward-shifted anomalous Aleutian Low, with consequent relative decreases of temperature over northern North America (i.e., reduced anomalous warming during future El Niño events), as well as relative decreases of temperature over the southeastern United States (i.e., greater anomalous cooling during El Niño events). These patterns are somewhat different for the models with future reductions of El Niño

amplitude because the changes of the anomalous Aleutian Low are not quite the same, with weakening in the A1B experiment, and an eastward shift in the 4XCO₂ experiment.

The changes in mean base state climate in the upper troposphere in the Northern Hemisphere midlatitudes with increases of GHGs, characterized by an anomalous wave-5 pattern as noted in previous studies, is present in the six models analyzed here, as well as in a larger number of available models. This base state climate change is consistent with the changes of El Niño teleconnections in the models with increased El Niño amplitude, but less so in the models with decreased El Niño amplitude. Therefore, it is likely that changes in base state as well as changes in future El Niño amplitude both are important for the changes in future El Niño teleconnections.

Analyses with greater numbers of models, such as illustrated in this study, provide better guidance concerning the issue of changes of El Niño teleconnections. Systematic errors of the El Niño simulations in the various models could contribute to whether the future events have greater

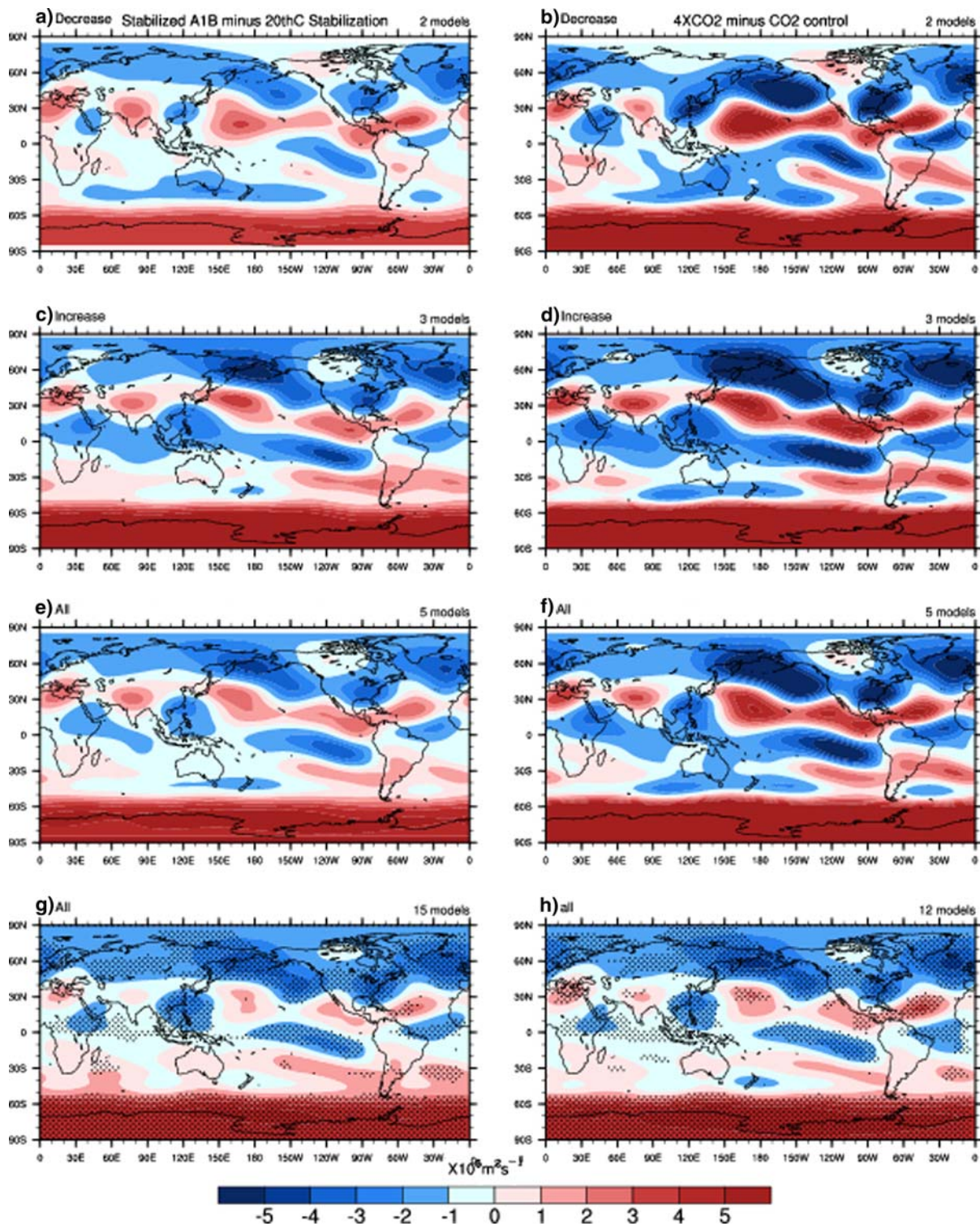


Fig. 8 a Differences of base state upper tropospheric circulation, 300 hPa streamfunction, stabilized A1B minus 20th century stabilization experiment for the two-member composite for models with projections of decreased El Niño amplitude (ECHO-G did not supply upper level winds); b same as a except for 4XCO₂ minus CO₂ control events; c same as a except for the three models with projected increases of El Niño amplitude; d same as b except for the three

models with projected increases of El Niño amplitude; e same as a except for the five-member multi-model ensemble; f same as b except for the five-member multi-model ensemble; g same as e except for a 15-member multi-model ensemble; h same as f except for a 12-member multi-model ensemble. In g and h *stippling* indicates more than 80% of the ensemble members agree on the sign of change in El Niño teleconnections

or smaller amplitude. However the very consistent change in midlatitude circulation has the largest effect on future El Niño teleconnections over North America. Systematic errors in the tropics appear to affect this pattern less than the manifestation of individual El Niño events in the respective models. Thus, the changed midlatitude base state with increasing CO₂ has the most consistent influence on the changes of El Niño teleconnections over North America, and also is the least model dependent.

Acknowledgments We acknowledge the modeling groups for making their simulations available for analysis, the Program for Climate Model Diagnosis and Intercomparison (PCMDI) for collecting and archiving the CMIP3 model output, and the WCRP's Working Group on Coupled Models (WGCM) for organizing the model data analysis activity. The WCRP CMIP3 multi-model dataset is supported by the Office of Science, U.S. Department of Energy. This work was supported in part by the Office of Science, U.S. Department of Energy, Cooperative Agreement No. DE-FC02-97ER62402, and by the Weather and Climate Impact Assessment Initiative at the National Center for Atmospheric Research. The National Center for Atmospheric Research is sponsored by the National Science Foundation.

References

- Achutarao K, Sperber K (2006) ENSO simulation in coupled ocean-atmosphere models: are the current models better? *Clim Dyn* 27. doi:10.1007/s00382-006-0119-7
- Arblaster JM, Meehl GA, Moore A (2002) Interdecadal modulation of Australian rainfall. *Clim Dyn* 18:519–531
- Branstator G, Haupt S (1998) An empirical model of barotropic atmospheric dynamics and its response to tropical forcing. *J Clim* 11:2645–2667
- Capotondi A, et al (2006) Spatial and temporal structure of ENSO in 20th century coupled simulations. *Ocean Model* 15(3–4):274–298
- Collins M (2000) The El Niño Southern oscillation in the second Hadley Centre coupled model and its response to greenhouse warming. *J Clim* 13:1299–1312
- Guilyardi E (2005) El Niño-mean state-seasonal cycle interactions in a multi-model ensemble. *Clim Dyn*. doi:10.1007/s00382-005-0084-6
- Guilyardi E, et al (2004) Representing El Niño in coupled ocean-atmosphere GCMs: the dominant role of the atmospheric component. *J Clim* 17:4623–4629
- Joseph R, Nigam S (2006) ENSO evolution and teleconnections in IPCC 20th century climate simulations: realistic representation? *J Clim* 19:4360–4377
- Knutson TR, Manabe S (1998) Model assessment of decadal variability and trends in the tropical Pacific Ocean. *J Clim* 11:2273–2296
- Meehl GA (1987) The annual cycle and interannual variability in the tropical Pacific and Indian Ocean regions. *Mon Weather Rev* 115:27–50
- Meehl GA, Branstator GW, Washington WM (1993) Tropical Pacific interannual variability and CO₂ climate change. *J Clim* 6:42–63
- Meehl GA, Washington WM, Collins WD, Arblaster JM, Hu A, Buja LE, Strand WG, Teng H (2005) How much more global warming and sea level rise? *Science* 307:1769–1772
- Meehl GA, Teng H, Branstator GW (2006) Future changes of El Niño in two global coupled climate models. *Clim Dyn*. doi:10.1007/s00382-005-0098-0
- Meehl GA, et al (2007a) Global climate projections. In: *Climate Change 2007: The Physical Science Basis. Contribution of Working Group I to the Fourth Assessment Report of the Intergovernmental Panel on Climate Change*, Cambridge University Press, Cambridge (in press)
- Meehl GA, Covey C, Delworth T, Latif M, McAvaney B, Mitchell JFB, Stouffer RJ, Taylor KE (2007b) The WCRP CMIP3 multi-model dataset: a new era in climate change research. *Bull Am Meteorol Soc* (in press)
- Merryfield W (2006) Changes to ENSO under CO₂ doubling in a multi-model ensemble. *J Clim* 19:4009–4027
- Rayner NA, Parker DE, Horton EB, Folland CK, Alexander LV, Rowell DP, Kent EC, Kaplan A (2003) Global analyses of sea surface temperature, sea ice, and night marine air temperature since the late nineteenth century. *J Geophys Res* 108(D14):4407. doi:10.1029/2002JD002670
- Selten FM, Branstator GW, Dijkstra HA, Kliphuis M (2004) Tropical origins for recent and future Northern Hemisphere climate change. *Geophys Res Lett* 31:L21205. doi:10.1029/2004GL020739
- Timmermann A (1999) Detecting the nonstationary response of ENSO to greenhouse warming. *J Atmos Sci* 56:2313–2325
- van Loon H, Meehl GA, Milliff R (2003) The Southern oscillation in the early 1990s. *Geophys Res Lett* 30. doi:10.1029/2002GL016307
- van Oldenborgh G, Philip S, Collins M (2005) El Niño in a changing climate: a multi-model study. *Ocean Sci Discuss* 2:267–298
- Yasunari T (1991) ‘‘The monsoon year’’—a new concept of the climatic year in the tropics. *Bull Am Meteorol Soc* 72:1331–1338